scientific reports

OPEN

Experimental study on the effects of blending PODE$_n$ on performance, combustion and emission characteristics of heavy-duty diesel engines meeting China VI emission standard

Yuwei Zhao[1]✉, Cong Geng[2], Weibo E[1], Xiaoquan Li[1], Peiyuan Cheng[1] & Tianlin Niu[1]

To study the influence of diesel fuel blended with polyoxymethylene dimethyl ethers (PODE$_n$), a new alternative fuel with a high oxygen content and large cetane number, on the combustion characteristics, fuel economies, and emission characteristics of heavy-duty diesel engines that meet China VI emission standards, relevant tests were conducted on a supercharged intercooled high-pressure common-rail diesel engine. The PODE$_n$ were blended with diesel fuel at three different ratios (volume fractions of 10%, 20%, and 30%). The test results showed that the PODE$_n$ could optimize the combustion process of diesel engines that met the China VI emission standards, effectively improve the thermal efficiencies of diesel engines, and reduce the emissions of hydrocarbon (HC), carbon monoxide (CO), and soot. With an increase in the PODE$_n$ blending ratio, the peak values of the in-cylinder pressure, average in-cylinder temperature, and instantaneous heat release rate gradually decreased, and each peak progressively moved forward. As the start of combustion gradually moved forward, the combustion duration was shortened by 0.7–2.8°CA, the heat release process became more concentrated, and the effective thermal efficiency was increased by up to 2.57%. The effective fuel consumption gradually increased, yet the equivalent effective fuel consumption gradually decreased, with the largest drop being as high as 4.55%. The nitrogen oxides (NO$_x$) emission increased slightly, and the emissions of HC, CO, and soot gradually decreased. The emissions of CO and soot declined significantly under high-speed and high-load conditions, with the highest reductions reaching 66.2% and 76.3%, respectively.

To address the environmental pollution and energy crises prevailing worldwide, countries around the world continue to implement increasingly stringent regulations related to the discharge of pollutants. The EU began to implement European VI, VI b, and VI c emission standards in January 2013, September 2014, and September 2017, respectively. Compared with the European V emission standard, the European VI emission standard contained added emission limits for the particle number (PN), and the on board diagnostics (OBD) limit was even more stringent. Proposed by the Environmental Protection Agency (EPA) in March 2013, the Tier 3 fuel and vehicle standards will be implemented in phases from 2017 to 2025. The EPA's Tier 3 limits the total emissions of "NMOG (nonmethane organic gas) + NO$_x$." China plans to fully implement the China VI a emission standards in 2020 and the China VI b emission standards in 2023. Shenzhen took the lead in implementing the China VI a emission standard at the end of 2018, while Shanghai, Guangzhou, Tianjin, and other cities began to enforce the China VI b emission standard on July 1, 2019. Formulated based on both the European VI c and EPA Tier 3 emission standards in terms of the requirements for the OBD and the evaporative emissions, the China VI emission standard is known as the strictest emission standard in the world.

[1]Air and Missile Defense College, Air Force Engineering University, Xi'an 710051, People's Republic of China. [2]College of Foreign Studies, Guilin University of Technology, Guilin 541004, People's Republic of China. ✉email: ywzhao1987@126.com

Diesel engines are widely used in transportation, agriculture, and industry[1–3]. Facing increasingly strict emissions regulations and a gradually growing energy crisis, investigators are pursuing the efficient and clean combustion of diesel. The optimization of fuel characteristics by blending oxygenated fuels is an effective way to achieve this objective[4–6]. Once the oxygenated fuel is blended with diesel, the physical and chemical properties of the blended fuel, e.g., the oxygen content, cetane number, and latent heat of evaporation, are changed accordingly, thereby altering the spray characteristics, combustion features, power performance, and emission characteristics of diesel engines[7–11]. Alcohols (e.g., methanol[12] and ethanol[13,14]), ethers (e.g., dimethyl ether[15]), and esters (e.g., biodiesel[16]) are currently the primary oxygenated fuels blended in diesel. Oxygenated fuels such as alcohols, ethers, and esters are strongly competitive for improving the combustion process and pollutant emissions of diesel engines. However, significantly different from diesel in terms of overall physical and chemical properties, these fuels are restricted in various ways in practical applications[17,18]. Therefore, it is of great practical significance to find oxygenated fuels with similar physical and chemical properties to those of diesel.

As a new type of oxygenated additive for diesel, polyoxymethylene dimethyl ethers ($PODE_n$) are chemically expressed as $CH_3O(CH_2O)_nCH_3$ (the degree of polymerization n is an integer, $2 \leq n \leq 8$). With physical and chemical properties fairly similar to those of diesel, $PODE_n$ are liquid at 20 °C and they can be miscible with diesel in any proportion. With a high oxygen content (45.2–51%), a large cetane number (above 63), and without a C–C bond in their molecular structure, $PODE_n$ are able to effectively reduce the soot emissions during the combustion process of diesel engines[19–22]. In addition, the production costs of $PODE_n$ are close to those of diesel, and with the advancement of production technology and the expanded production scale of $PODE_n$, the production costs of $PODE_n$ are expected to be further reduced, which makes it possible for $PODE_n$ to be applied to diesel engines on a large scale. Hence, $PODE_n$ are a type of clean alternative fuel that exhibit excellent performances and great potential[23–30].

Recently, a number of studies have been carried out to study the effects of blending $PODE_n$ into diesel on diesel engines with different emission standards. By fueling a light-duty diesel vehicle with the Euro II emission standard using diesel blended with 10% $PODE_n$, Pellegrini et al.[31] reduced the particulate matter (PM) emissions by 18%, while if pure $PODE_n$ were used, the PM emissions could be decreased by 77%, meeting the Euro IV emission standard. By blending 7.5% $PODE_n$ into the diesel used on a Euro III light-duty diesel engine, Pellegrini et al.[32] found that compared with pure diesel, diesel blended with $PODE_n$ reduced the PM emissions and the exhaust smoke by 13% and 32%, respectively, with increased emissions of polycyclic aromatic hydrocarbons (PAHs) and PM with particle sizes smaller than 30 nm. Liu et al.[33] burned diesel blended with 15% and 25% $PODE_n$ in a Euro IV diesel engine, indicating that blending $PODE_n$ could significantly improve the trade-off relationship between the emissions of NO_x and the soot of the diesel engine. Under the WHSC test cycle, with the NO_x emissions controlled at 2.7 g/(kW·h), the soot emissions met the Euro VI emission standard. Liu et al.[34] studied the effect of the $PODE_n$ blending ratio on the performance of a diesel engine with China IV emission standards, and the results showed that as the $PODE_n$ blending ratio increased, the ignition delay period shortened, the in-cylinder temperature gradually increased, the soot emission was reduced by up to 47.6%, and the effective thermal efficiency could be increased by up to 3.4%. Wang et al.[35,36] explored the impact of blending $PODE_n$ on the combustion and emission characteristics of light-duty and heavy-duty diesel engines, and the results indicated that blending $PODE_n$ prolonged the ignition delay period and increased the peak heat release of the main injection. When 20% $PODE_n$ were blended, the soot and CO emissions of a light-duty diesel engine could be reduced by 90%, the PM emissions of a heavy-duty diesel engine during the ESC (European Stationary Cycle) test cycle were reduced by 36.2%, and the effective thermal efficiency was increased by 0.85%. Moreover, to further improve the physical and chemical properties of fuels, Huang et al.[37] and Chen et al.[38] studied a ternary fuel mixture of diesel, $PODE_n$, and high-octane fuel, and the results indicated that blending a certain proportion of $PODE_n$ in the diesel or high-octane fuel could reduce the emissions of NO_x and soot.

Therefore, blending $PODE_n$ can effectively improve the combustion and emission characteristics of diesel engines, especially when it comes to reducing the emissions of soot and PM. It also has been shown that the same fuel has different combustion and emission performances in different types of diesel engines[39]. Likewise, there are certain differences in the effects of blending the same proportion of $PODE_n$ into the diesel fuel on the combustion characteristics of different types or models of engines as well as the effects on the emissions of NO_x, soot, and CO[26,31,34,36,40,41]. Many studies have confirmed the feasibility of adding $PODE_n$ to diesel engines, yet there are few experimental studies regarding $PODE_n$ blending with the diesel used in diesel engines that meet the China VI emission standards. Given that China is about to fully implement the China VI emission standards, it is necessary to carry out such studies on $PODE_n$/diesel blended fuels with China VI diesel engines. To this end, with a supercharged, intercooled, high-pressure common-rail diesel engine with the China VI emission standards as the research subject, the influences of the $PODE_n$ blending ratio on the combustion and emission characteristics as well as the fuel economy of a heavy-duty diesel engine were investigated in this study. The results will provide empirical support for optimizing the fuel characteristics and combustion process of $PODE_n$ as an alternative fuel for China VI emission standards and the revision of the release control and post-treatment strategies.

Materials and methods

Testing apparatus.
A Weichai Power WP12.460 China VI heavy-duty diesel engine, an in-line 6-cylinder, supercharged, intercooled, electronically controlled high-pressure common-rail diesel engine was used in the tests. The technical specifications of the engine are shown in Table 1.

The testing apparatus was mainly composed of an electric eddy current dynamometer, a combustion analyzer, a mass flow meter, a coolant and oil thermostatic system, and an exhaust gas analyzer. Figure 1 shows the schematic layout of the testing apparatus. The Kistler6052C cylinder pressure sensor was used to collect the in-cylinder pressure, which was amplified and recorded by the Kistler5064 charge amplifier built inside the KiBox

2

Parameter	Specifications
Engine type	In-line 6-cylinder, 4-stroke, supercharged, intercooled, high-pressure common-rail
Bore × stroke (mm × mm)	126 × 155
Compression ratio	17
Displacement (L)	11.596
Rated power (kW)	338
Rated speed (r·min⁻¹)	1900
Fuel injection system	Bosch CRSN2-16

**Table 1.** Technical specifications of the diesel engine.
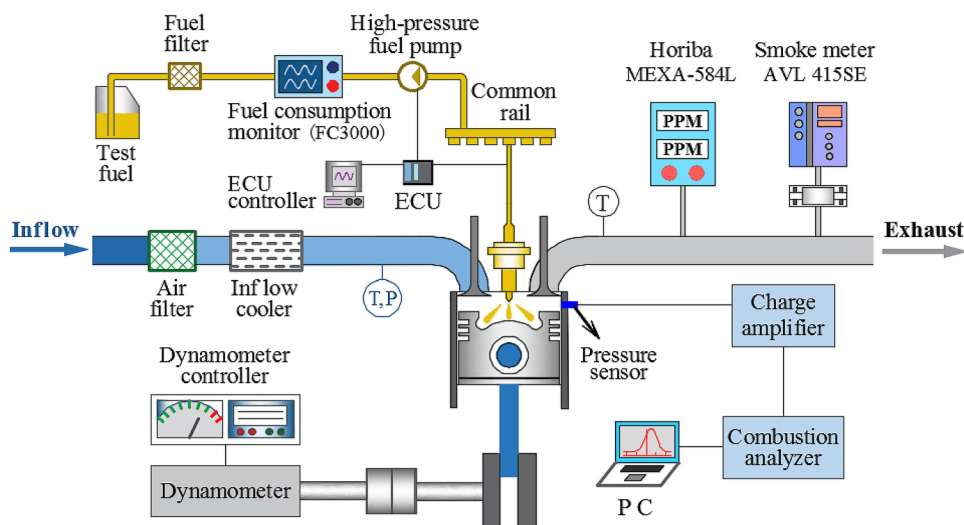
Figure 1. Schematic diagram of the testing apparatus.

Properties	Diesel	PODE$_n$	P10D90	P20D80	P30D70
Cetane number	56.5	78.6	58.71	60.92	63.13
Low heat value (MJ·kg⁻¹)	42.5	19.05	39.76	37.11	34.57
Oxygen mass fraction (%)	0	46.98	5.49	10.79	15.89
Density at 25 °C (g·cm⁻³)	0.855	1.02	0.872	0.888	0.905
Kinematic viscosity at 25 °C (cSt)	3.44	1.05	3.16	2.89	2.63
Boiling point (°C)	188	158.49	184.55	181.22	178.02

Table 2. Physical and chemical parameters of the fuels.

combustion analyzer. The heat release rate and the other combustion characteristics data were calculated by the KiBox combustion analyzer. The Horiba MEXA-584L exhaust gas analyzer was used to measure the emissions of NO_x, HC, and CO, and the AVL 415SE smoke meter was used to measure the exhaust soot. The Siemens FC3000 mass flow meter was used to measure the fuel consumption.

Testing fuels. The PODE$_n$ used in the study were industrial PODE$_n$ with a purity of 99.9% that were produced by Shandong Yuhuang Chemical (Group) Co., Ltd., and they were primarily composed of PODE$_2$, PODE$_3$, and PODE$_4$ with mass fractions of 2.553%, 88.9%, and 8.48%, respectively. The test diesel was 0# commercial diesel. In this test, three kinds of PODE$_n$/diesel blended fuels were prepared, with PODE$_n$ volume percentages of 10%, 20%, and 30%, which were denoted as P10D90, P20D80, and P30D70, respectively, and the pure diesel was denoted as P0D100. The physical and chemical properties of the fuel are shown in Table 2. The physical and chemical properties of P10D90, P20D80, and P30D70 were calculated based on Eqs. (1) and (2) from a previous study[42].
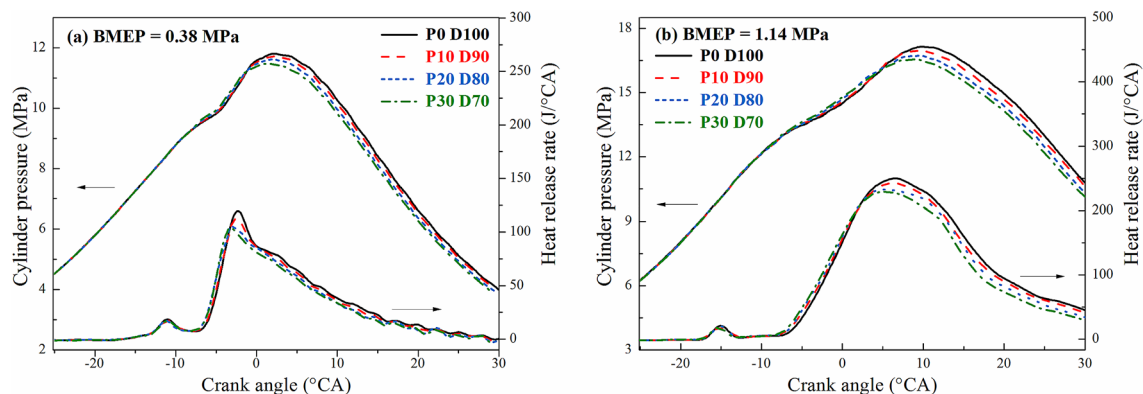
Figure 2. Effects of PODE$_n$ blending ratio on in-cylinder pressure and instantaneous heat release rate.

Testing protocol. Four different loads under two speeds, i.e., n = 1300 and 2000 r·min^{-1}, were tested, with brake mean effective pressure (BMEP) values of 0.38 MPa, 0.76 MPa, 1.14 MPa, and 1.52 MPa. During the test, except for the fuel blend, the fuel injection strategy and the other control parameters remained constant, and the exhaust gas recirculation (EGR) valve remained closed. Under different operating conditions, the fuel injection strategy was the two-stage injection of the original machine: "pre-injection + main injection," and the injection time and pressure were based on those of the original machine. Both the cooling water temperature and the oil temperature were controlled at about 80 °C. The ambient temperature for the test was 22 °C ± 3 °C, and the atmospheric humidity was 10% ± 3%.

Prior to the tests, all the instruments and the equipment were calibrated to ensure the reliability of the test and the accuracy of the test results. During the test, each operating point was repeatedly measured to eliminate uncertainty. After the engine was operating stably for 5 min, the fuel consumption was measured three times, and the average value was taken as the test result. The combustion analyzer collected the combustion character-istics data for 200 cycles and the average value of the data was taken for analysis. The exhaust gas analyzer and the smoke meter continued to be measured for 1 min, and with the invalid values eliminated, the average values were taken as the test results.

Results and discussion

Effects of blending PODE$_n$ on combustion characteristics of diesel engines.

Figure 2 shows the variation of the in-cylinder pressure and instantaneous heat release rate of the diesel engine with differ-ent PODE$_n$ blending ratios when n = 2000 r·min^{-1}, BMEP = 0.38 MPa, and BMEP = 1.14 MPa. Since the fuel injection consisted of two stages, the exothermic process was divided into two phases: pre-injection and main-injection heat release. Since the pre-injection lasted for a relatively short time, the amounts of fuel injection and heat released were small, and the blending of the PODE$_n$ exerted no significant effect on the peak value of the pre-injection heat release rate. However, since the duration of the main-injection phase was longer, the peak value of the main-injection heat release rate decreased with the increase in the PODE$_n$ blending ratio, with the peak phase gradually moving forward. Because the PODE$_n$ had a lower heat value than diesel, under the injec-tion conditions controlled by the electronic control unit (ECU) of the original engine, the blended fuel emitted less heat than the diesel with a declining peak value of the heat release rate. Moreover, the PODE$_n$ had a large cetane number, which shortened the ignition delay period of the blended fuel and advanced the ignition timing.

Figure 2 also shows that as the PODE$_n$ blending ratio increased, the maximum in-cylinder pressure decreased, with the corresponding phase of the peak in-cylinder pressure gradually moving forward. Due to the large cetane number, great self-ignitability, and good volatility of the PODE$_n$, the ignition delay period of the blended fuel became shorter, with the corresponding phase of the peak in-cylinder pressure moving forward. The peak in-cylinder pressure decreased due to the following two factors. First, the lower heat value of the PODE$_n$ reduced the heat value of the blended fuel and the heat release during the main-injection phase. Second, the shortening of the ignition delay period of the blended fuel caused the start of combustion (SOC) to occur earlier, shortened the mixing time of the fuel and the air, and reduced the premixed combustion ratio.

Figure 3 shows the variation of the average in-cylinder temperature with different PODE$_n$ blending ratios when n = 2,000 r·min^{-1}, BMEP = 0.38 MPa, and BMEP = 1.14 MPa. As the PODE$_n$ blending ratio increased, the peak in-cylinder temperature dropped and the curve shifted forward. Since the latent heat of vaporization of the blended fuel increased after the blending of the PODE$_n$, after the fuel was injected into the cylinder, part of the heat was absorbed, resulting in a relatively significant temperature drop, which led to a decrease in the peak in-cylinder temperature. However, due to the large cetane number of the PODE$_n$, the combustion heat release of the blended fuel was advanced, thereby shifting the peak in-cylinder temperature forward.

Figure 4 shows the variation of the combustion duration of the engine with different PODE$_n$ blending ratios when n = 2,000 r·min^{-1}, BMEP = 0.38 MPa, and BMEP = 1.14 MPa. In this study, the crank angle corresponding to a cumulative heat release rate of 10% (CA10) was defined as the SOC, the crank angle corresponding to a cumulative heat release rate of 90% (CA90) was defined as the end of combustion (EOC), and the crank angle between the SOC and the EOC was defined as the combustion duration. With BMEP = 1.14 MPa, compared with
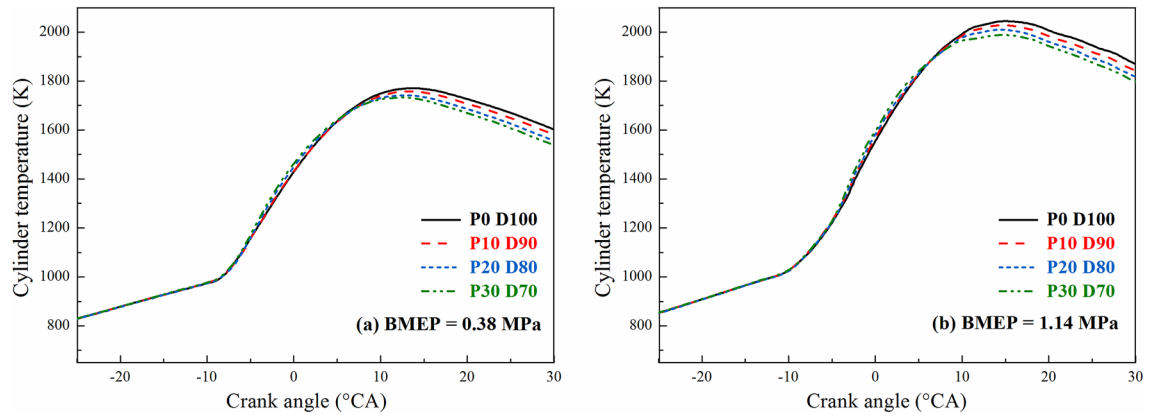
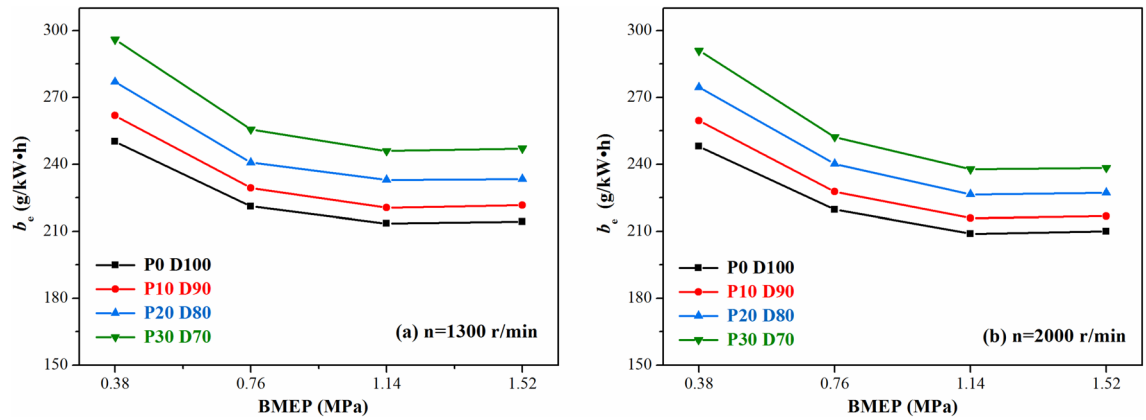**Figure 3.** Effects of $PODE_n$ blending ratio on in-cylinder temperature.
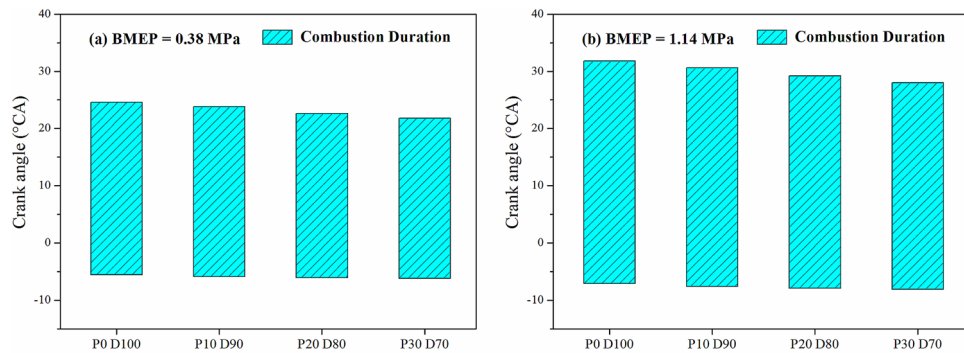
Figure 4. Effects of $PODE_n$ blending ratio on combustion duration.
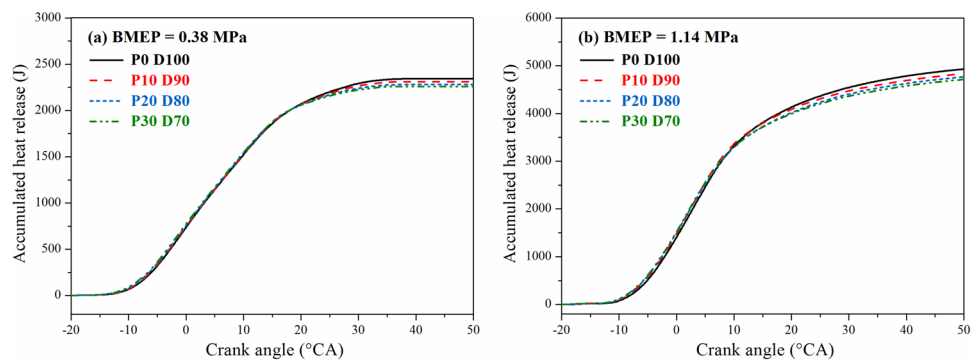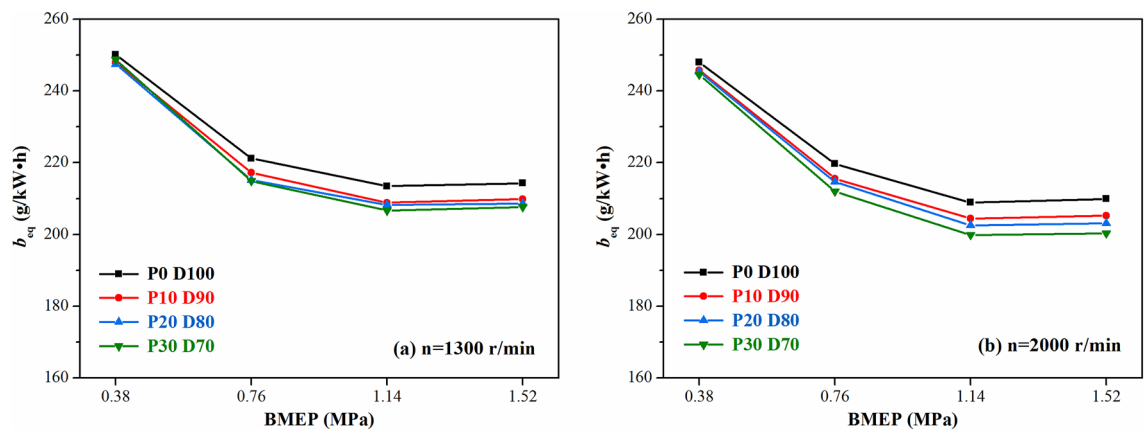

Figure 5. Effects of $PODE_n$ blending ratio on cumulative heat release.

P0D100, when P10D90, P20D80, and P30D70 were used, the CA10 was advanced by 0.5°CA, 0.8°CA, and 1.0°CA, respectively, and the CA90 was advanced by 1.2°CA, 2.6°CA, and 3.8°CA, respectively, and the combustion duration was shortened by 0.7°CA, 1.8°CA, and 2.8°CA, respectively. This indicated that as the $PODE_n$ blending ratio increased, the combustion duration was gradually shortened, and the heat release was more concentrated, which was conducive to improving the thermal efficiency of the engine.

Figure 5 shows the variation of the cumulative heat release of the engine with different $PODE_n$ blending ratios when n = 2,000 r·min⁻¹, BMEP = 0.38 MPa, and BMEP = 1.14 MPa. The cumulative heat release decreased after the $PODE_n$ were blended, and with the increase in the blending ratio, the cumulative heat dropped more significantly. At a BMEP of 1.14 MPa, when P0D100, P10D90, P20D80, and P30D70 were used, the maximum cumulative amounts of heat released were 4,959.9 J, 4,863.6 J, 4,789.1 J, and 4,733.6 J, respectively. Compared with P0D100, the cumulative amounts of heat released were reduced by 1.94%, 3.44%, and 4.56% when P10D90, P20D80, and P30D70 were burned, respectively. At the same speed and load, the effective power values of the

Figure 6. Effects of PODE$_n$ blending ratio on effective fuel consumption.

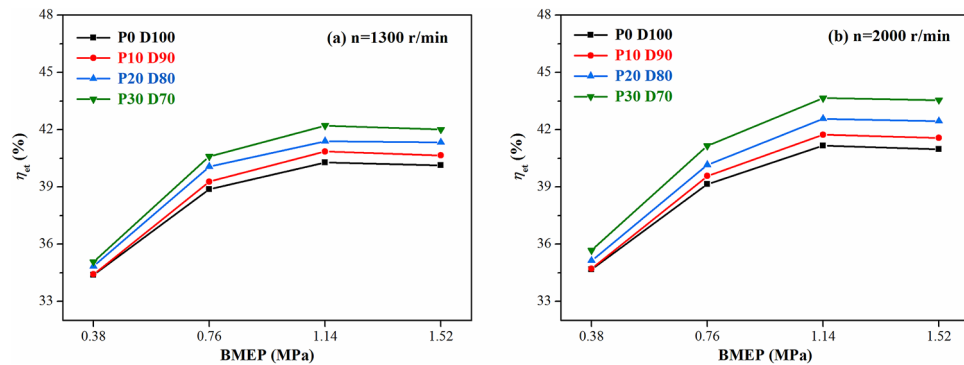**Figure 7.** Effects of PODE$_n$ blending ratio on equivalent effective fuel consumption.

engine were equal for all the blends. The lower the cumulative heat release was, the higher the thermal efficiency of the engine was. This indicated that blending PODE$_n$ helped to improve the effective thermal efficiency of the engine. This conclusion is further discussed in "Effects of blending PODE$_n$ on fuel economy of diesel engines".

Effects of blending PODE$_n$ on fuel economy of diesel engines. The effective fuel consumption b_e and the effective thermal efficiency η_{et} are two important parameters that characterize the fuel economy of the engine, and they are critical indicators for measuring the engine performance. Because the low heat value of PODE$_n$ differs greatly from that of diesel, directly comparing the fuel consumption of the fuels could not accurately reflect the total heat consumed by the fuels. Therefore, the concept of equivalent effective fuel consumption b_{eq} was introduced; i.e., the total heat value consumed by the PODE$_n$/diesel blended fuel was converted to the diesel consumption corresponding to an equivalent heat value.

The variations of the effective fuel consumption b_e with different PODE$_n$ blending ratios are shown in Fig. 6. Given the same speed and load, the effective fuel consumption gradually increased with the increase in the PODE$_n$ blending ratio. Due to the low heat value of the PODE$_n$, the heat values of the blended fuels P10D90, P20D80, and P30D70 were 93.6%, 87.3%, and 81.3% of that of diesel, respectively, and the amount of heat released by combustion within the unit mass of the blended fuel was reduced. Without changing the fuel injection strategy, the output torques corresponding to the same BMEP operating condition were the same. Hence, it was important to increase the injection amount of the blended fuel, resulting in an increase in the effective fuel consumption.

Figures 7 and 8 show the variations of the equivalent effective fuel consumption b_{eq} and the effective thermal efficiency η_{et} of the engine with different PODE$_n$ blending ratios. Given the same load, with the increase in the PODE$_n$ blending ratio, the equivalent effective fuel consumption gradually decreased, and the effective thermal efficiency increased significantly. With n = 2000 r·min^{-1} and BMEP = 1.52 MPa, compared with P0D100, the equivalent effective fuel consumptions of P10D90, P20D80, and P30D70 decreased by 2.20%, 3.26%, and 4.55%, respectively, with the effective thermal efficiencies increasing by 0.59%, 1.48%, and 2.57%, respectively. Due to the large cetane number of the PODE$_n$, once the PODE$_n$ were blended, the ignition delay period was shortened, and the combustion advanced with the heat release and the peak in-cylinder pressure in the main-injection phase being closer to the top dead center (Fig. 2), which was conducive to the improvement of the thermal efficiency. Furthermore, once the PODE$_n$ were blended, the combustion duration shortened (Fig. 4), the heat released

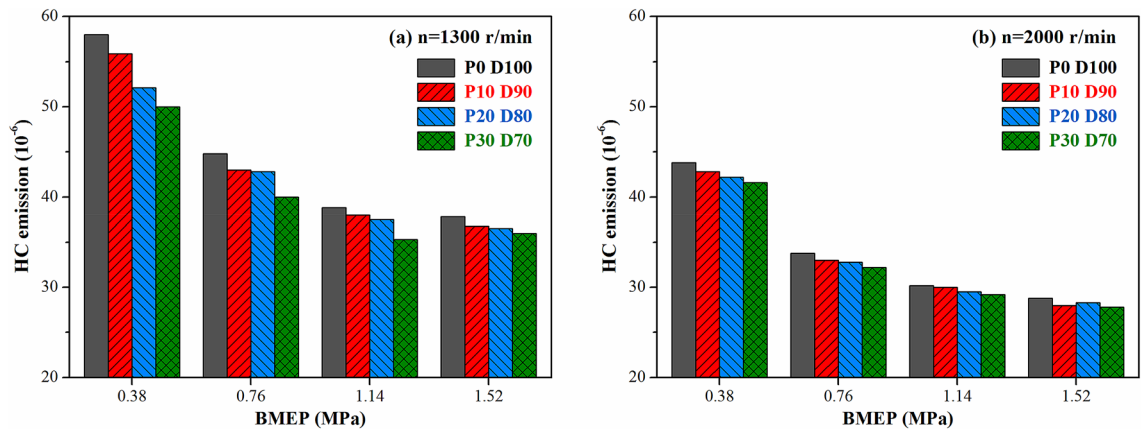**Figure 8.** Effects of PODE$_n$ blending ratio on effective thermal efficiency.
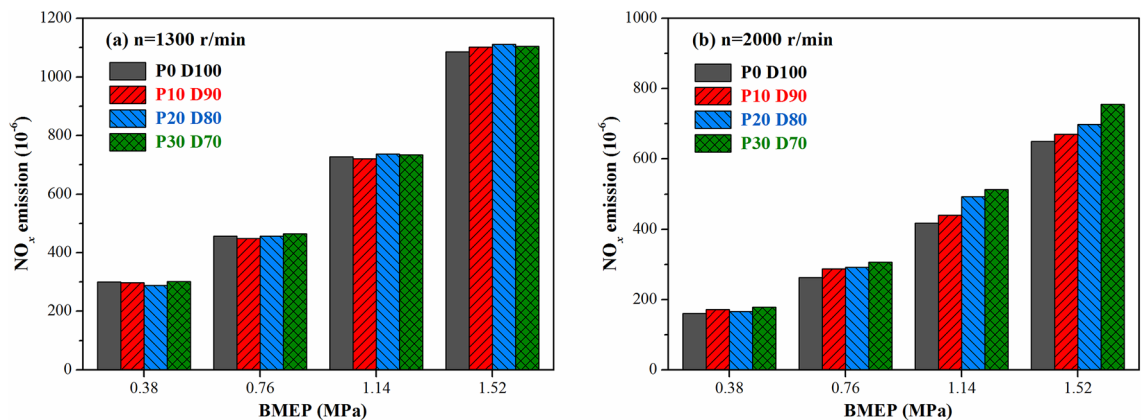
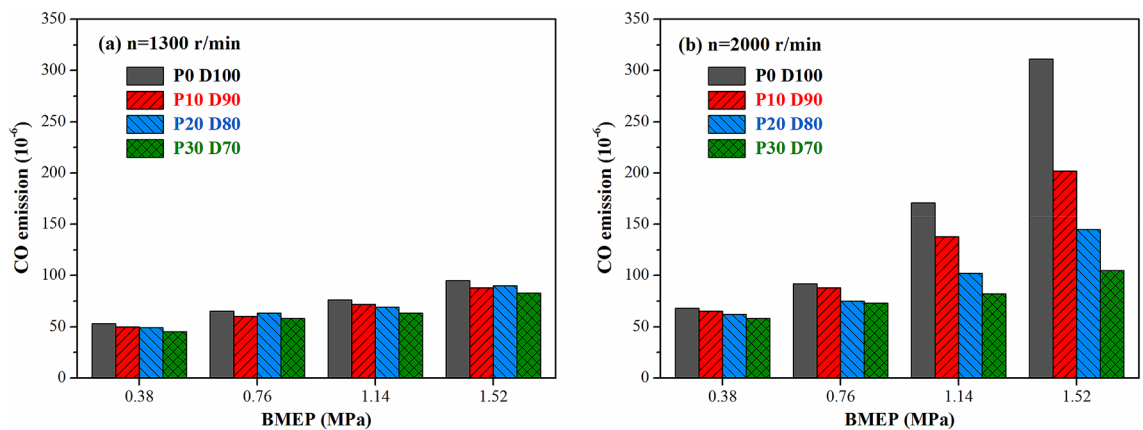**Figure 9.** Effects of PODE$_n$ blending ratio on NO$_x$ emission.

became more concentrated, and the low in-cylinder temperature (Fig. 3) reduced the heat transfer loss. Furthermore, with the increase in the PODE$_n$ blending ratio, the oxygen content in the blended fuel increased, which reduced the area of oxygen-deficient combustion and improved the combustion reaction speed. In summary, blending PODE$_n$ effectively improved the effective thermal efficiency of the engine and reduced the equivalent effective fuel consumption.

Effects of blending PODE$_n$ on emission characteristics of diesel engines. High-temperature and oxygen-rich conditions with a long high-temperature duration are required for the formation of NO$_x$[43]. Figure 9 shows the effect of the PODE$_n$ blending on the engine emission of NO$_x$ under different operating conditions. Under low-speed conditions (n = 1300 r·min^{-1}), the in-cylinder temperature was low. As the PODE$_n$ blending ratio increased, the in-cylinder temperature further declined (Fig. 3). Moreover, the shortened combustion duration shortened the high-temperature duration and suppressed the generation of NO$_x$. However, the increased oxygen content in the high-temperature region increased the emission of NO$_x$. Combining the two effects, blending PODE$_n$ into the diesel fuel at different ratios made little difference under low-speed conditions. Under high-speed conditions (n = 2000 r·min^{-1}), the in-cylinder temperature increased rapidly. Although blending PODE$_n$ decreased the in-cylinder temperature, the in-cylinder temperature remained high (the peak temperature shown in Fig. 3 was about 2000 K). At that time, the NO$_x$ was quite sensitive to the oxygen concentration in the cylinder during combustion, so the high oxygen content of the PODE$_n$ rapidly increased the emission of NO$_x$. In addition, the NO$_x$ emission at a speed of 2,000 r·min^{-1} was generally lower than that at 1,300 r·min^{-1}, which was likely because after the speed increased, the fuel reaction time was reduced, the high-temperature duration decreased, and the emission of NO$_x$ decreased. At the same speed, as the load increased, the emission of NO$_x$ increased due to the increase in the in-cylinder temperature.

The effect of PODE$_n$ blending on the HC emission of the engine under different operating conditions is shown in Fig. 10. With n = 1,300 r·min^{-1}, with the increase in the PODE$_n$ blending ratio, the emission of HC gradually decreased. This was because the emissions of HC were mainly generated in the lean gas mixture and wall quenching layer around the injection fuel spray. The large cetane number of the PODE$_n$ improved the ignition performance of the blended fuel and shortened the ignition delay period, thereby reducing the HC emission in the lean gas mixture and wall quenching layer. Moreover, due to the low boiling point and high oxygen content of the PODE$_n$, the speed of mixing and combustion of oil and gas improved, which was beneficial for the oxidation

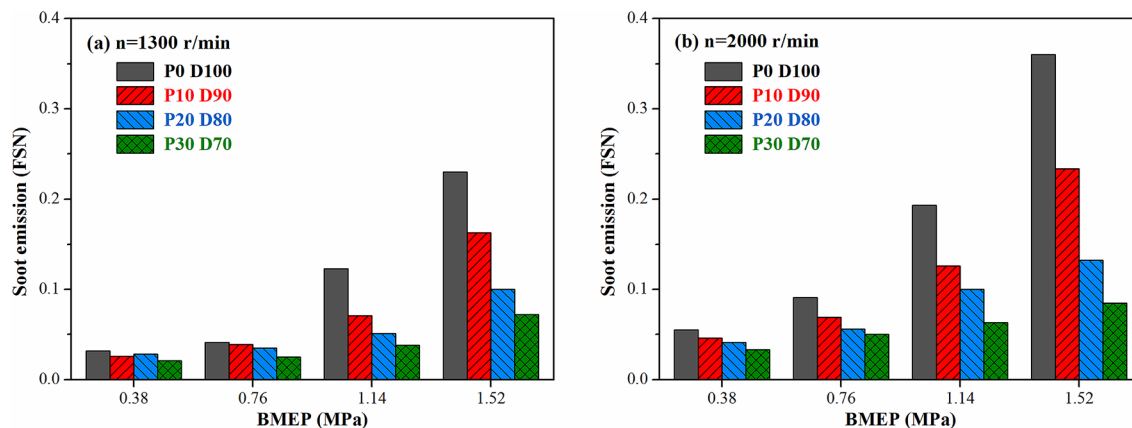**Figure 10.** Effects of $PODE_n$ blending ratio on HC emission.

Figure 11. Effects of $PODE_n$ blending ratio on CO emission.

of HC. With n = 2,000 r·min^{-1}, the in-cylinder temperature was relatively high, and the emission of HC was low and decreased slightly with the increase in the $PODE_n$ blending ratio. As the load increased, the emission of HC significantly decreased. This was because as the load increased, the in-cylinder temperature gradually increased, more HC was oxidized, and the emission of HC gradually decreased.

The emission of CO was mainly generated in rich mixed gas areas or low-temperature areas where the excess air coefficient was less than 1. Figure 11 shows the effect of $PODE_n$ blending on the CO emission of the engine under different operating conditions. At a speed of 1,300 r·min^{-1}, the emission of CO was quite low when different fuels were used, and the emission changed slightly as the load increased. Since the excess air coefficient was large at low speeds, the emission of CO was comparatively low. At a speed of 2,000 r·min^{-1}, the emission of CO declined slightly with the increase in the $PODE_n$ blending ratio at low and medium loads, whereas at high loads, the emission of CO decreased significantly as the $PODE_n$ blending ratio increased. With BMEP = 1.52 MPa, the CO emissions of P10D90, P20D80, and P30D70 were reduced by 35.0%, 53.4%, and 66.2%, respectively, compared with that of P0D100. At low and medium loads, the diesel engine basically worked with lean mixtures with an excess air coefficient greater than 1. There were fewer low-temperature and hypoxic areas in the cylinder, and the emission of CO was relatively low. Thus, the $PODE_n$ had a comparatively small impact on the emission of CO. At high loads, there was a relatively rich mixture of local hypoxia in the cylinder, resulting in a rapid increase in the emission of CO. The high oxygen content of $PODE_n$ increased the air–fuel ratio and excess air coefficient, improved the combustion conditions in the local hypoxic areas in the combustion chamber, and accelerated the oxidation rate of CO, which significantly decreased the emission of CO.

Figure 12 shows the effect of $PODE_n$ blending on the soot emission under different operating conditions. Blending $PODE_n$ could effectively reduce the soot emission of diesel engines, and the reduction was more evident under large loads. With n = 2,000 r·min^{-1} and BMEP = 1.52 MPa, the filter smoke number (FSN) values of P10D90, P20D80, and P30D70 decreased by 35.1%, 62.8%, and 76.3% compared to that of P0D100. Unlike diesel, the $PODE_n$ exhibited great volatility and a low viscosity and boiling point. Therefore, blending $PODE_n$ contributed to the evaporation and atomization of the fuel, improved the homogeneity of the mixed gas, and effectively avoided fuel cracking caused by an uneven gas mixture under high-temperature and hypoxia conditions[44]. Furthermore, blending $PODE_n$ increased the oxygen content in the blended fuel, which supplied the oxygen during the combustion process, thereby improving the combustion conditions in some areas during

Figure 12. Effects of PODE$_n$ blending ratio on soot emission.

the diffusion combustion process of the diesel engine and promoting the post-oxidation process of the soot. In particular, the PODE$_n$ molecules did not contain C–C bonds, which could significantly reduce the amounts of olefins and PAHs generated during the combustion reaction, thereby lowering the amount of soot. The above factors greatly improved the soot emission of the diesel engine after the blending of PODE$_n$. Furthermore, under high speeds and loads, the soot emission decreased more substantially with the increase in the PODE$_n$ blending ratio. With increases in the speed and the load, the combustion temperature in the cylinder increased, and the high-temperature hypoxic areas increased. Hence, due to the high oxygen content and excellent volatility, the PODE$_n$ had a more evident effect on improving the combustion conditions when the gas mixture had an excessively high concentration.

Conclusions

PODE$_n$, with a high oxygen content and a large cetane number, are a promising additive for diesel. In this study, a series of tests were performed on a supercharged intercooled high-pressure common-rail diesel engine powered by diesel fuel blended with PODE$_n$ at different ratios, i.e., 10%, 20%, and 30%, to explore the influences of PODE$_n$ blending on the combustion and emission characteristics as well as the fuel economies of a heavy-duty diesel engine that met the China VI emission standards. The following conclusions were obtained:

(1) Blending PODE$_n$ significantly affected the combustion characteristics of the diesel engine. As the PODE$_n$ blending ratio increased, the peak in-cylinder pressure and the average in-cylinder temperature gradually decreased, and the phase corresponding to the peak gradually shifted forward. The peak heat release rate in the pre-injection stage varied slightly, and the peak heat release rate in the main-injection stage gradually decreased, with the phase corresponding to the peak gradually moving forward.

(2) As the PODE$_n$ blending ratio increased, the start of the combustion gradually shifted forward, the duration of combustion was shortened by 0.7–2.8°CA, the heat release became more concentrated, the combustion heat release of the fuel was closer to the top dead center, and the maximum effective thermal efficiency could be improved by 2.57%. After blending with PODE$_n$, the effective fuel consumption increased, but the equivalent effective fuel consumption decreased significantly, with the maximum reduction reaching 4.55%.

(3) Blending PODE$_n$ into diesel could effectively improve the emission characteristics of the diesel engines. Particularly under high-speed and high-load conditions, the PODE$_n$, due to its high oxygen content and great volatility, improved the oxygen concentration in the cylinder and the uniformity of the combustible mixture, which effectively inhibited the generation of soot and reduced the emission of soot by as much as 76.3%. With the increase in the PODE$_n$ blending ratio, the emission of NO$_x$ increased slightly, but the emissions of HC and CO gradually decreased, with the highest reduction of the CO emissions reaching 66.2%.

References

1. Gao, J. B., Chen, H. B., Tian, G. H., Ma, C. C. & Zhu, F. An analysis of energy flow in a turbocharged diesel engine of a heavy truck and potentials of improving fuel economy and reducing exhaust emissions. *Energy Convers. Manag.* **184**, 456–465 (2019).
2. Liu, Y. & Tan, J. Experimental study on solid SCR technology to reduce NO$_x$ emissions from diesel engines. *IEEE Access* **8**, 151106–151115 (2020).
3. Dimitriadis, A. *et al.* Improving PM-NO$_x$ trade-off with paraffinic fuels: A study towards diesel engine optimization with HVO. *Fuel* **265**, 116921 (2020).
4. Omari, A., Heuser, B., Pischinger, S. & Rüdinger, C. Potential of long-chain oxymethylene ether and oxymethylene ether-diesel blends for ultra-low emission engines. *Appl. Energ.* **239**, 1242–1249 (2019).

5. Zare, A. *et al.* Diesel engine emissions with oxygenated fuels: A comparative study into cold-start and hot-start operation. *J. Clean. Prod.* **162**, 997–1008 (2017).
6. Tang, Q., Liu, H., Ran, X., Li, M. & Yao, M. Effects of direct-injection fuel types and proportion on late-injection reactivity controlled compression ignition. *Combust. Flame* **211**, 445–455 (2020).
7. Amid, S. *et al.* Effects of waste-derived ethylene glycol diacetate as a novel oxygenated additive on performance and emission characteristics of a diesel engine fueled with diesel/biodiesel blends. *Energy Convers. Manag.* **203**, 112245 (2020).
8. Hosseinis, H., Alisaraeia, T., Ghobadian, B. & Mayvan, A. Performance and emission characteristics of a CI engine fueled with carbon nanotubes and diesel-biodiesel blends. *Renew. Energy* **111**, 201–213 (2017).
9. Guan, C., Cheung, C. S., Li, X. L. & Huang, Z. Effects of oxygenated fuels on the particle-phase compounds emitted from a diesel engine. *Atmos. Pollut. Res.* **8**, 209–220 (2017).
10. Rodríguez-Fernández, J., Hernández, J. J. & Sánchez-Valdepeñas, J. Effect of oxygenated and paraffinic alternative diesel fuels on soot reactivity and implications on DPF regeneration. *Fuel* **185**, 460–467 (2016).
11. Liu, J. *et al.* Compound combustion and pollutant emissions characteristics of a common-rail engine with ethanol homogeneous charge and polyoxymethylene dimethyl ethers injection. *Appl. Energy* **239**, 1154–1162 (2019).
12. Yasin, M. H. M., Yusaf, T., Mamat, R. & Yusop, A. F. Characterization of a diesel engine operating with a small proportion of methanol as a fuel additive in biodiesel blend. *Appl. Energy* **114**, 865–873 (2014).
13. Pedrozo, V. B., May, I., Nora, M. D., Cairns, A. & Zhao, H. Experimental analysis of ethanol dual-fuel combustion in a heavy-duty diesel engine: An optimisation at low load. *Appl. Energy* **165**, 166–182 (2016).
14. Yang, X., Huang, X., Zhang, W., Wei, P. & Xu, S. Comparisons of the emissions of ethanol/diesel and n-pentanol/diesel fuel blends: engine test and kinetic modeling study. *IEEE Access* **7**, 106213–106224 (2019).
15. Theinnoi, K., Suksompong, P. & Temwutthikun, W. Engine performance of dual fuel operation with in-cylinder injected diesel fuels and in-port injected DME. *Energy Proc.* **142**, 461–467 (2017).
16. Wang, Y., Liu, H. & Lee, C. F. F. Particulate matter emission characteristics of diesel engines with biodiesel or biodiesel blending: A review. *Renew. Sust. Energ. Rev.* **64**, 569–581 (2016).
17. Pachiannan, T. *et al.* A literature review of fuel effects on performance and emission characteristics of low-temperature combustion strategies. *Appl. Energy* **251**, 113380 (2019).
18. Fang, Q., Fang, J., Zhuang, J. & Huang, Z. Effects of ethanol-diesel-biodiesel blends on combustion and emissions in premixed low temperature combustion. *Appl. Therm. Eng.* **54**, 541–548 (2013).
19. Awad, O. I. *et al.* Overview of polyoxymethylene dimethyl ether additive as an eco-friendly fuel for an internal combustion engine: Current application and environmental impacts. *Sci. Total Environ.* **715**, 136849 (2020).
20. Liu, J. *et al.* Effects of PODE/diesel blends on particulate matter emission and particle oxidation characteristics of a common-rail diesel engine. *Fuel Process. Technol.* **212**, 106634 (2021).
21. O'Connell, N., Roll, A., Lechner, R., Luo, T. & Brautsch, M. PODE-blend as pilot fuel in a biomethane dual fuel engine: Experimental analysis of performance, combustion and emissions characteristics. *Renew. Energ* **143**, 101–111 (2019).
22. Li, B. *et al.* Combustion and emission characteristics of diesel engine fueled with biodiesel/PODE blends. *Appl. Energy* **206**, 425–431 (2017).
23. Zhang, Z. *et al.* Effect of soybean oil/PODE/ethanol blends on combustion and emissions on a heavy-duty diesel engine. *Fuel* **288**, 119625 (2021).
24. Liu, H. *et al.* Combustion and emission characteristics of a direct injection diesel engine fueled with biodiesel and PODE/biodiesel fuel blends. *Fuel* **209**, 62–68 (2017).
25. Liu, H. *et al.* Effect of diesel/PODE/ethanol blends on combustion and emissions of a heavy duty diesel engine. *Fuel* **257**, 116064 (2019).
26. Chen, H., Huang, R., Huang, H. Z., Pan, M. Z. & Teng, W. W. Potential improvement in particulate matter's emissions reduction from diesel engine by addition of PODE and injection parameters. *Appl. Therm. Eng.* **150**, 591–604 (2019).
27. Duraisamy, G., Rangasamy, M. & Govindan, N. A comparative study on methanol/diesel and methanol/ PODE dual fuel RCCI combustion in an automotive diesel engine. *Renew. Energ* **145**, 542–556 (2020).
28. Zhao, Y. W. *et al.* Energy balance analysis, combustion characteristics, and particulate number concentration-NO_x trade-off of a heavy-duty diesel engine fueled with various $PODE_n$/diesel blends. *Energy Convers. Manag.* **225**, 113489 (2020).
29. Duraisamy, G., Rangasamy, M. & Govindan, N. A comparative study on methanol/diesel and methanol/PODE dual fuel RCCI combustion in an automotive diesel engine. *Renew. Energy* **145**, 542–556 (2020).
30. Lin, Q. J. *et al.* Polyoxymethylene dimethyl ether 3 (PODE3) as an alternative fuel to reduce aerosol pollution. *J. Clean Prod.* **285**, 124857 (2021).
31. Pellegrini, L.; Marchionna, M.; Patrini, R.; Florio, S. Emission performance of neat and blended polyoxymethylene dimethyl ethers in an old light-duty diesel car. *SAE Tech. Paper* **2013**, 2013–01–1035.
32. Pellegrini, L.; Patrini, R.; Marchionna, M. Effect of POMDME blend on PAH emissions and particulate size distribution from an in-use light-duty diesel engine. *SAE Tech. Paper* **2014**, 2014–01–1951.
33. Liu, J. L. *et al.* Effects of diesel/PODE (polyoxymethylene dimethyl ethers) blends on combustion and emission characteristics in a heavy duty diesel engine. *Fuel* **177**, 206–216 (2016).
34. Liu, J. H., Sun, P., Huang, H., Meng, J. & Yao, X. H. Experimental investigation on performance, combustion and emission characteristics of a common-rail diesel engine fueled with polyoxymethylene dimethyl ethers-diesel blends. *Appl. Energy* **202**, 527–536 (2017).
35. Wang, Z., Liu, H. Y., Zhang, J., Wang, J. X. & Shuai, S. J. Performance, combustion and emission characteristics of a diesel engine fueled with polyoxymethylene dimethyl ethers ($PODE_{3-4}$)/diesel blends. *Energy Proc.* **75**, 2337–2344 (2015).
36. Liu, H. Y., Wang, Z., Zhang, J., Wang, J. X. & Shuai, S. J. Study on combustion and emission characteristics of polyoxymethylene dimethyl ethers/diesel blends in light-duty and heavy-duty diesel engines. *Appl. Energy* **185**, 1393–1402 (2017).
37. Huang, H. Z. *et al.* Influence of n-butanol-diesel-$PODE_{3-4}$ fuels coupled pilot injection strategy on combustion and emission characteristics of diesel engine. *Fuel* **236**, 313–324 (2019).
38. Chen, H., Su, X., Li, J. H. & Zhong, X. L. Effects of gasoline and polyoxymethylene dimethyl ethers blending in diesel on the combustion and emission of a common rail diesel engine. *Energy* **171**, 981–999 (2019).
39. Chen, Z. B. *et al.* Experimental investigation of the performance and emissions of diesel engines by a novel emulsified diesel fuel. *Energy Convers. Manag.* **95**, 334–341 (2015).
40. Gao, W., Liu, J., Sun, P., Yang, C. & Fang, J. Gaseous emissions and particle microstructure characteristics of PODE/diesel blend fuel. *Int. J. Automot. Technol.* **20**(3), 607–617 (2019).
41. Wang, T. *et al.* Influence of injection parameters on combustion, gaseous emissions and particle size distribution of a CRDI diesel engine operating with PODE/diesel blends. *Fuel* **281**, 118733 (2020).
42. Wang, J. X., Wu, F. J., Xiao, J. H. & Shuai, S. J. Oxygenated blend design and its effects on reducing diesel particulate emissions. *Fuel* **88**, 2037–2045 (2009).
43. Heywood, J. B. *Internal Combustion Engine Fundamentals* 586–592 (McGraw-Hill, 1988).
44. Chen, L. F., Liang, Z. R., Liu, H. Y., Ding, S. R. & Li, Y. F. Sensitivity analysis of fuel types and operational parameters on the particulate matter emissions from an aviation piston engine burning heavy fuels. *Fuel* **202**, 520–528 (2017).

Author contributions

Funding

Competing interests

The authors declare no competing interests.

Additional information

Correspondence and requests for materials should be addressed to Y.Z.

Reprints and permissions information is available at www.nature.com/reprints.

Publisher's note Springer Nature remains neutral with regard to jurisdictional claims in published maps and institutional affiliations.